Early cluster evolution

Star Cluster Formation: Mapping the first few Myr
Grenoble Aug.29-31 2018

31st Aug 2018

Pavel Kroupa

Helmholtz-Institute for Radiation und Nuclear Physics (HISKP)

University of Bonn

c/o Argelander-Institut für Astronomie

Astronomical Institute,

Charles University in Prague

Initial cluster radii & the expansion problem

Pavel Kroupa: University of Bonn & Charles University

Very young star clusters are typically very compact, < 1pc

Open star clusters (age > few 10 Myr) have typical half-mass radii near 3 pc

This size difference constrains the formation of star clusters :

Monolithic molecular cloud core collapse
or
~~hierarchical merging of smaller clusters~~

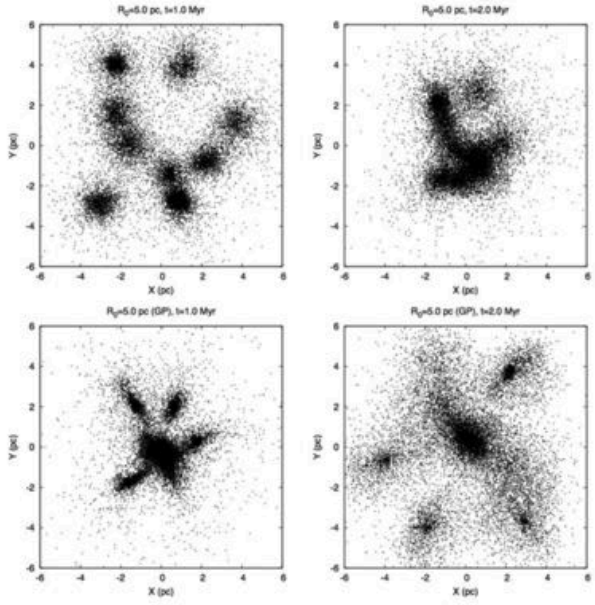

Figure 7. Evolution for the 'extended' system A-IIId ($R_0 = 5$ pc, see Table 3). As expected, the infall of the subclusters proceeds much more slowly than that for the compact systems (cf. Figs 4). The system is still highly substructured (SUB) at $t \approx 2.0$ Myr both in absence (panels 1,2, numbered left-to-right, top-to-bottom) and presence (panels 3,4) of a gas potential. In presence of the gas potential, the subclusters are close to the first arrival at their pericentres (i.e. $t \approx t_{in}$, see Section 3.1) at $t \approx 1$ Myr (panel 3) while this takes $t \approx 2$ Myr without the gas (panel 2). This is consistent with Fig. 3. For the evolution with gas potential, the subclusters make their first passage through each other during 1–2 Myr which is why their configuration at 2 Myr (panel 4) is more extended than that in 1 Myr (panel 3). Note that the gas potential tidally elongates the subclusters significantly (also see Fig. 8).

Banerjee & Kroupa 2015

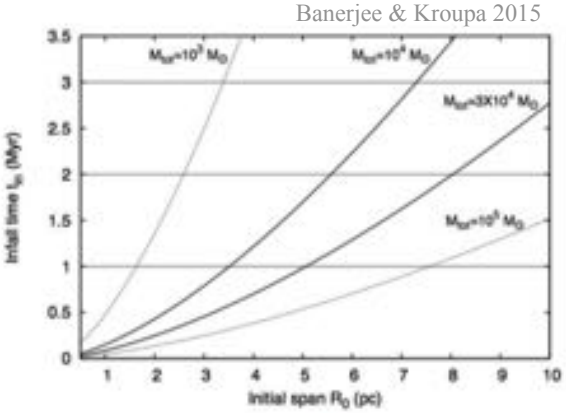

Figure 3. The infall time (or the time of first arrival at orbital pericentre, see Section 3.1) of the subclusters, t_{in}, as a function of the radius, R_0, of the spherical volume over which they are initially distributed. The curves are according to equation (2) for different systemic mass M_{tot}. For the present calculations, $M_{tot} = M_* = 10^4\ M_\odot$ without a residual gas and $M_{tot} = 3M_* = 3 \times 10^4\ M_\odot$ with the residual gas (see Section 2.2). These two curves are highlighted.

The typical present-day density (10^4–$10^5 M_\odot$ pc^{-3}; or size ≈1 pc), age (≈1–3 Myr) and (near) spherical core-halo morphology of gas-free very young massive clusters (VYMCs), like R136, NGC 3603 and the ONC, dictate an episodic or monolithic (or near monolithic) formation of such star clusters, undergoing a violent gas dispersal phase.

Banerjee & Kroupa, Chapter 6, in The Birth of Star Clusters, Stahler, ed. 2018

A&A 543, A8 (2012)
DOI: 10.1051/0004-6361/201118231

Astronomy & Astrophysics

Inverse dynamical population synthesis

Constraining the initial conditions of young stellar clusters by studying their binary populations

M. Marks[1,2,*] and P. Kroupa[1]

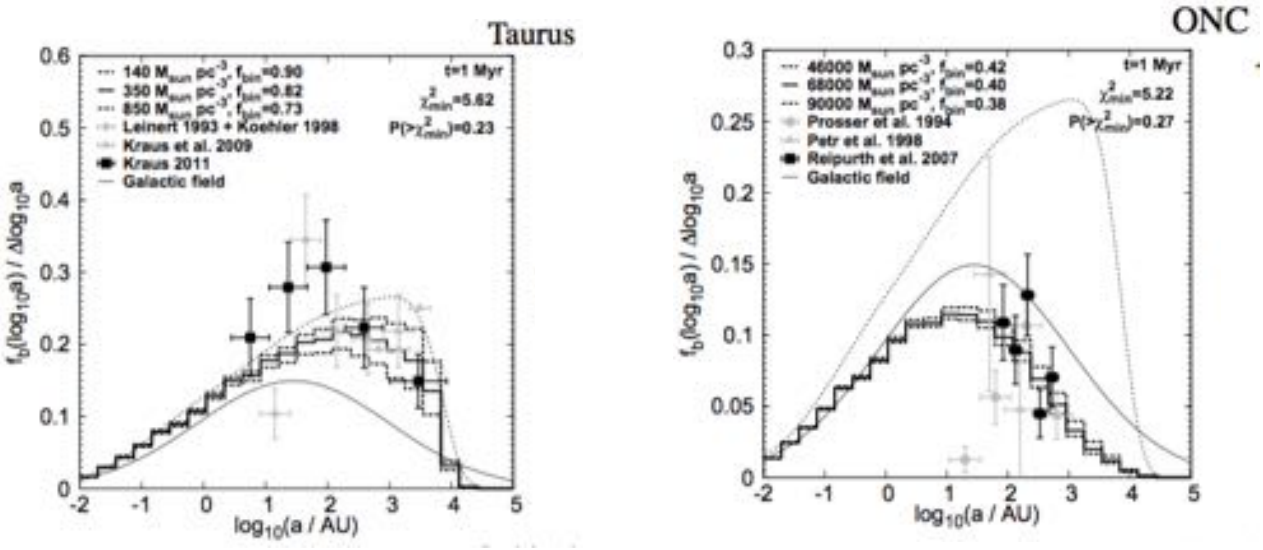

Marks & Kroupa 2012

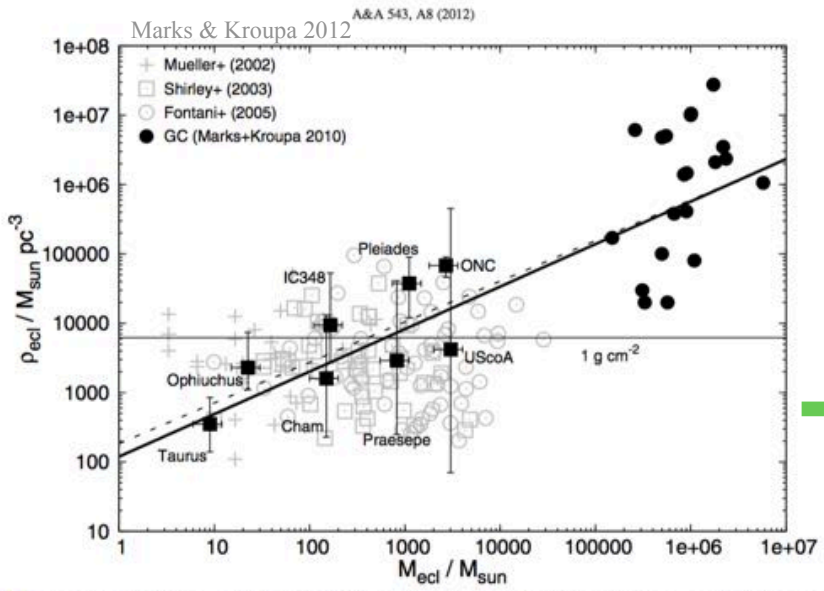

Fig. 6. Constraints on the initial volume-densities within the half-mass radius and masses derived in this work for the seven clusters (filled squares) versus the initial stellar mass. The indicated errors in mass correspond to the observationally inferred present-day mass on the left end of a bar and two times the present-day mass on its right end, to be understood as an estimator of the possible initial-mass range. Filled circles are Galactic GCs as in Fig. 5. Underlaid as grey symbols are data of molecular cloud clumps of Mueller et al. (2002, crosses), Shirley et al. (2003, squares), and Fontani et al. (2005, circles) as collated by Parmentier & Kroupa (2011). These are known to have already begun forming stars. The clump masses have been multiplied with a star-formation efficiency of one-third to compare to the stellar masses and densities inferred in the present work. The thin solid black-line is the threshold for massive-star formation evaluated by Krumholz & McKee (2008, 1 g cm^{-2}, see the text). The thick solid black-line is a least squares fit to both the young cluster and GC data (Eq. (6)), implying that there is a mass-radius relation (Eq. (7)) for star cluster-forming cloud clumps. The dashed line shows the result when the GCs are excluded from the fit.

$$\frac{r_h}{\mathrm{pc}} = 0.1 \left(\frac{M_{\mathrm{ecl}}}{M_\odot} \right)^{0.13}$$

Thus a consistent (using different arguments) picture emerges: stars form in very compact embedded clusters

$$r_h < 1\,\mathrm{pc}$$

Evidence from molecular clouds

Andre et al. 2014, Protostars and Planets VI

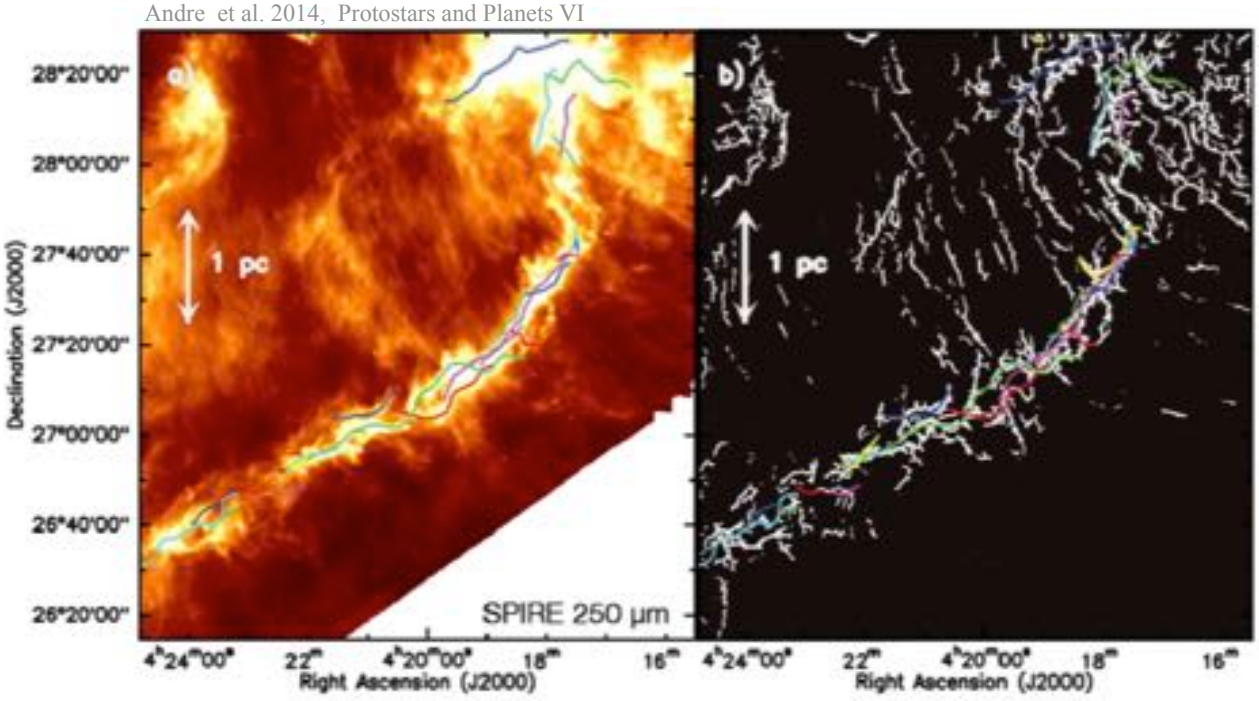

Fig. 2.— **(a)** *Herschel*/SPIRE 250 μm dust continuum image of the B211/B213/L1495 region in Taurus (*Palmeirim et al.*, 2013). The colored curves display the velocity-coherent "fibers" identified within the B213/B211 filament by *Hacar et al.* (2013) using $C^{18}O(1–0)$ observations. **(b)** Fine structure of the *Herschel*/SPIRE 250 μm dust continuum emission from the B211/B213 filament obtained by applying the multi-scale algorithm *getfilaments* (*Men'shchikov*, 2013) to the 250 μm image shown in panel (a). Note the faint striations perpendicular to the main filament and the excellent correspondence between the small-scale structure of the dust continuum filament and the bundle of velocity-coherent fibers traced by *Hacar et al.* (2013) in $C^{18}O$ (same colored curves as in (a)).

Pavel Kroupa: University of Bonn & Charles University

Andre et al. 2014, Protostars and Planets VI

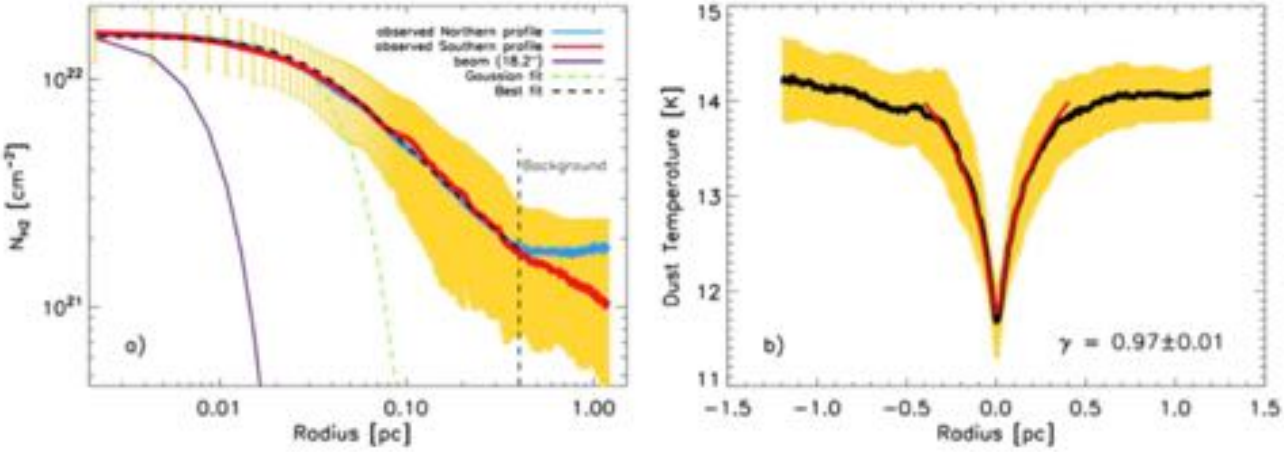

Fig. 4.— **(a)** Mean radial column density profile observed perpendicular to the B213/B211 filament in Taurus (*Palmeirim et al.*, 2013), for both the Northern (blue curve) and the Southern part (red curve) of the filament. The yellow area shows the ($\pm 1\sigma$) dispersion of the distribution of radial profiles along the filament. The inner solid purple curve shows the effective 18″ HPBW resolution (0.012 pc at 140 pc) of the *Herschel* column density map used to construct the profile. The dashed black curve shows the best-fit Plummer model (convolved with the 18″ beam) described by Eq. (1) with p=2.0±0.4 and a diameter $2 \times R_{\rm flat} = 0.07 \pm 0.01$ pc, which matches the data very well for $r \leq 0.4$ pc, **(b)** Mean dust temperature profile measured perpendicular to the B213/B211 filament in Taurus. The solid red curve shows the best polytropic model temperature profile obtained by assuming $T_{\rm gas} = T_{\rm dust}$ and that the filament has a density profile given by the Plummer model shown in the left panel (with $p = 2$) and obeys a polytropic equation of state, $P \propto \rho^{\gamma}$ [and thus $T(r) \propto \rho(r)^{(\gamma-1)}$]. This best fit corresponds to a polytropic index γ=0.97±0.01 (see *Palmeirim et al.*, 2013 for further details).

Andre et al. 2014, Protostars and Planets VI

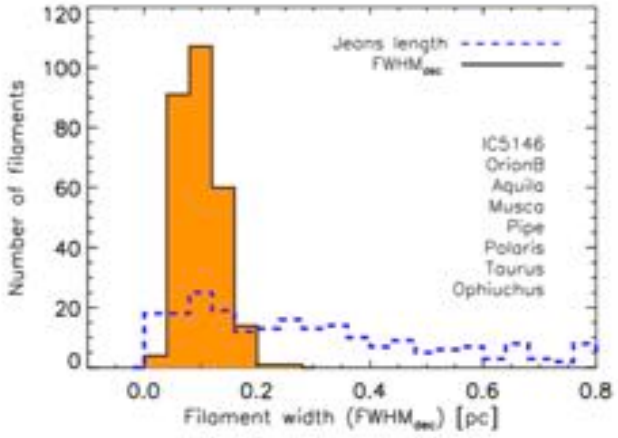

Fig. 5.— Histogram of deconvolved FWHM widths for a sample of 278 filaments in 8 nearby regions of the Gould Belt, all observed with *Herschel* (at resolutions ranging from $\sim$ 0.01 pc to $\sim$ 0.04 pc) and analyzed in the same way (*Arzoumanian et al.*, in prep. – see *Arzoumanian et al.*, 2011 for initial results on a subsample of 90 filaments in 3 clouds). The distribution of filament widths is narrow with a median value of 0.09 pc and a standard deviation of 0.04 pc (equal to the bin size). In contrast, the distribution of Jeans lengths corresponding to the central column densities of the filaments (blue dashed histogram) is much broader.

Remember fror the binary-star analysis :

$$\frac{r_h}{\rm pc} = 0.1 \left(\frac{M_{\rm ecl}}{M_\odot} \right)^{0.13}$$

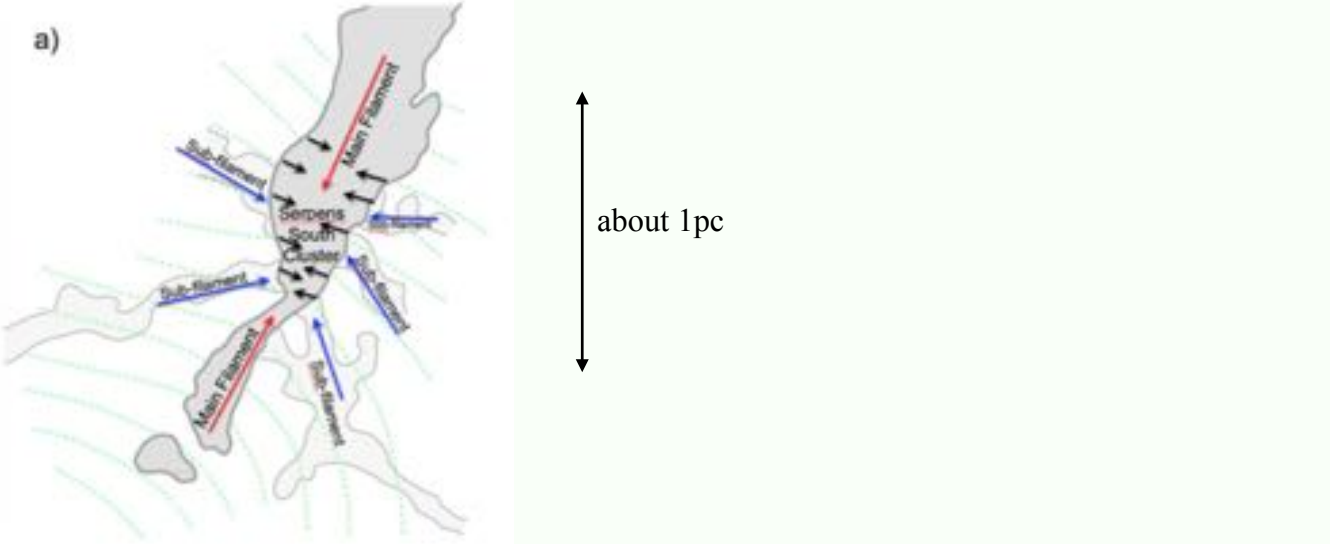

Fig. 9.— **(a)** Sketch of the typical velocity field inferred from line observations (e.g., *H. Kirk et al.*, 2013) within and around a supercritical filament (here Serpens-South in the Aquila complex – adapted from *Sugitani et al.*, 2011): Red arrows mark longitudinal infall along the main filament; black arrows indicate radial contraction motions; and blue arrows mark accretion of background cloud material through striations or subfilaments, along magnetic field lines (green dotted lines from *Sugitani et al.*).

Thus a consistent (using different arguments) picture emerges :
stars form in very compact embedded clusters

$r_h < 1\,\mathrm{pc}$ ✓

Very young star clusters are typically very compact, < 1pc

Open star clusters (age > few 10 Myr) have typical half-mass radii near 3 pc

This size difference constrains the formation of star clusters :

The cluster expansion problem

Banerjee & Kroupa 2017

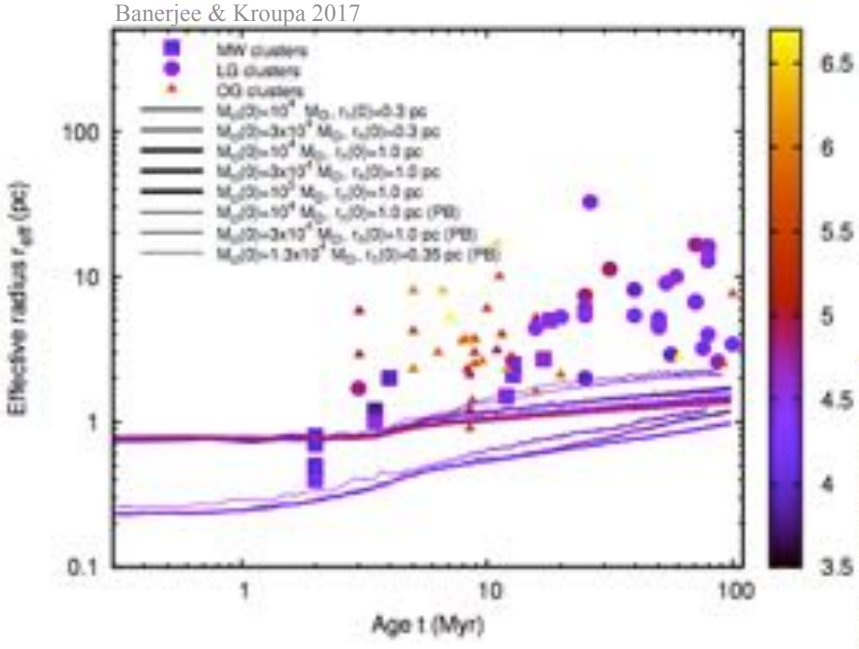

Fig. 3. *Top*: effective radius $r_{\rm eff}$ vs. age t for young massive bound star clusters (YMCs) in the Milky Way, the Local Group, and external galaxies which are distinguished by different filled symbols. The symbols are colour-coded according to the clusters' respective photometric mass, $\log_{10}(M_{\rm phot}/M_\odot)$. These observed data are given in Table 1. Overlaid in the panel are the computed curves for the evolution of projected half-mass radius (or effective radius) $r_{\rm eff}(t)$ for model star clusters with initial masses $M_{\rm cl}(0)$ and half-mass radii $r_{\rm h}(0)$ as given in Table 3, which do not include a residual gas expulsion phase. These curves are distinguished according to the legends in the panel where "PB" indicates that the computed cluster includes a realistic primordial binary population (see Sect. 2.1). These lines are also colour-coded according to the corresponding clusters' instantaneous total bound mass $\log_{10}(M_{\rm cl}(t)/M_\odot)$. As can be seen, if the clusters evolve from compact sizes determined by substructures in molecular clouds, their secular expansion substantially falls short of the observed sizes of YMCs (see text). *Bottom*: here, the

Very young embedded clusters can only expand sufficiently through the expulsion of about 60--70 % of their mass,

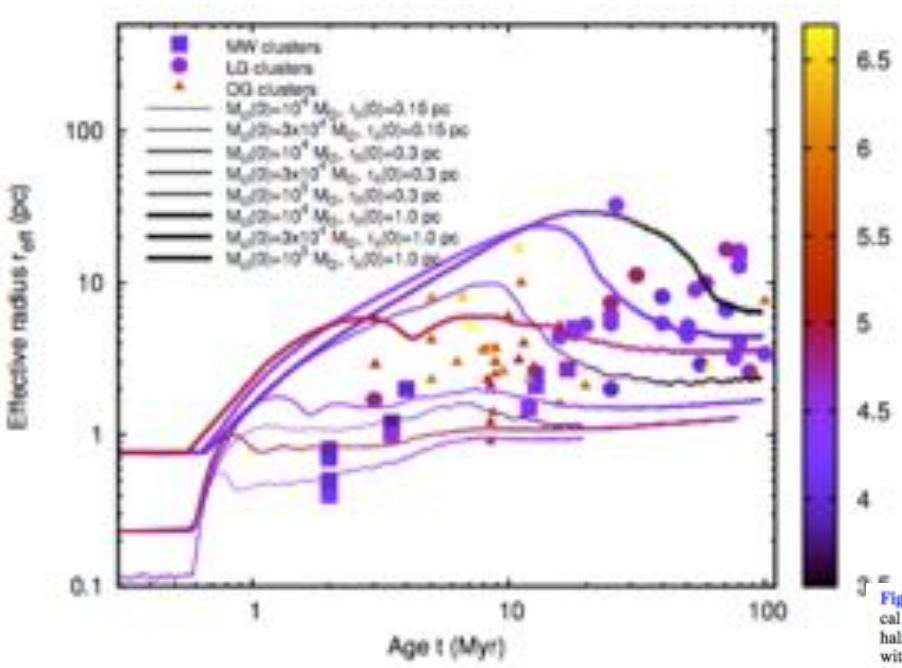

that is, if the $SFE \approx \frac{1}{3}$

But can this work ?

is there enough feedback energy?

Fig. 6. Data points and their colour-coding in both panels are identical to Fig. 3. The curves are the computed evolution of the projected half-mass radii (or effective radii) $r_{\rm eff}(t)$, including a gas dispersal phase with star formation efficiency $\epsilon \approx 33\%$ (see Table 4, top part and text for details). As in Fig. 3, the curves also follow the same colour-coding according to the corresponding clusters' instantaneous total bound mass $\log_{10}(M_{\rm cl}(t))$ (the same set of curves are overlaid on both panels). These figures imply that even if the YMCs evolve from filament-like compact sizes, such substantial (and explosive) gas dispersal will expand them to their present observed sizes (half-mass radii) in the Milky way and in the Local Group (*top panel*). However, to reach the sizes of the most extended Local Group YMCs, they need to evolve from $r_{\rm h}(0) \geq 1$ pc half-mass radii, unless such objects are low-mass cluster complexes (Brüns et al. 2009). The latter is also true for the young massive associations (*bottom panel*). See text for details.

The star-formation efficiency

Star clusters form from gas :

Only a fraction of the gas in the cluster volume forms stars :

star-formation efficiency

$$\epsilon = \frac{M_{\rm ecl}}{M_{\rm ecl}+M_{\rm gas}} \lesssim 0.4$$

(*eg.* Lada & Lada 2003; Megeath et al. 2016; ATLASGAL results/James Urquhart)

$\epsilon_{\rm obs} \leq 40\%$ (Lada & Lada 2003; Megeath et al. 2016) :

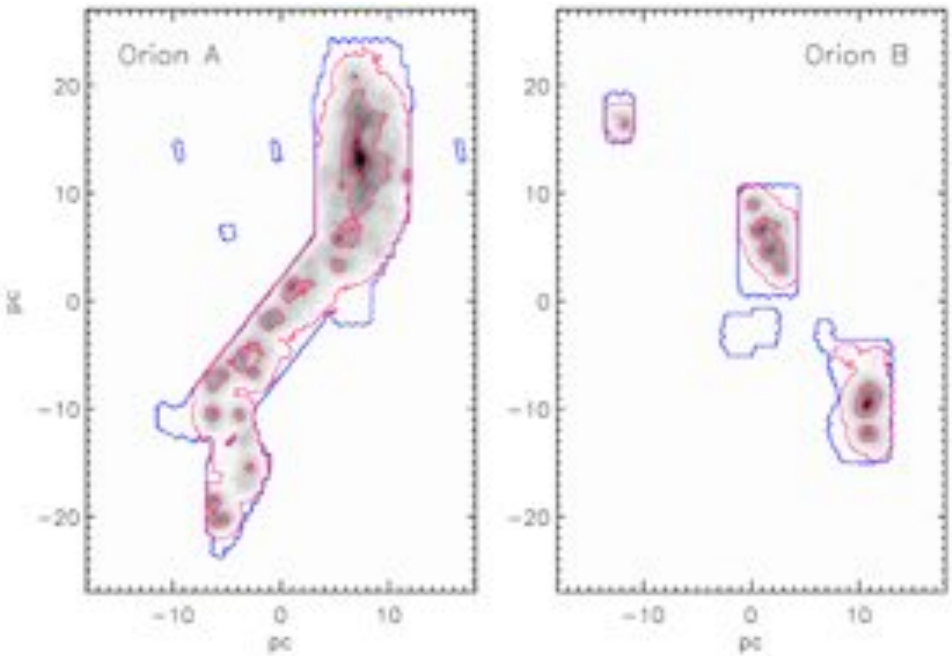

Megeath et al. 2016

Figure 8. Maps of the nearest neighbor surface density in the Orion A and B molecular clouds. We have used the 10th nearest neighbor and have corrected the densities for incompleteness. The blue contour gives the outline of the IRAC field. The inverted gray scale images renders the densities with a logarithmic scaling. The red contours are for 1, 10 and 100 YSOs pc^{-2}. The adopted distance is 414 pc.

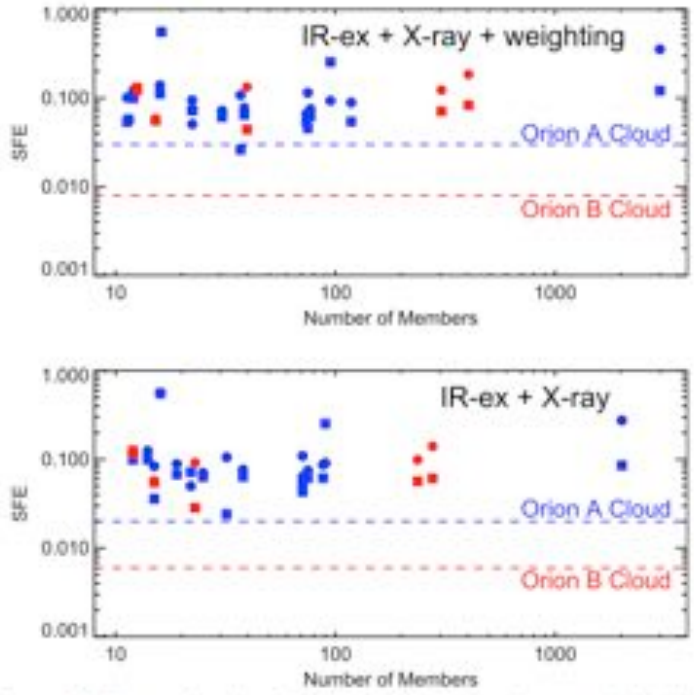

Figure 25. The star formation efficiency of the groups, clusters and clouds in the Orion complex with the blue symbols denoting regions within Orion A and the red symbols denoting regions within Orion B. The circles show the values determined for clusters and groups with the extinction map of Gutermuth et al. (2011) while the squares give the values determined from the ^{13}CO maps from Ripple et al. (2013). The dashed lines give the SFE for the entire Orion A and B clouds using total cloud masses from Wilson et al. (2005) and Lombardi et al. (2011). The upper panel uses the number dusty YSO corrected for incompleteness by both the application of the weighting correction and the inclusion of X-ray sources in the ONC and NGC 2024 clusters. The lower panel uses the number of detected dusty YSO augmented by the inclusion of X-ray sources and therefore gives systematically lower values.

Megeath et al. 2016

$\epsilon_{\rm obs} < 0.4$

The gas-removal time scale

How rapidly can the gas be expelled ?

$$E_{\rm bin} = \frac{GM_{\rm cl+g}^2}{R_0} = 8.6\times10^{40}\left(\frac{M_{\rm cl+g}}{M_\odot}\right)^2 \ {\rm erg}$$

$$t_{\rm cross} = 4.8\left(\frac{100\,M_\odot}{M_{\rm cl+g}}\right)^{\frac{1}{2}}\left(\frac{R_0}{\rm pc}\right)^{\frac{3}{2}}, \quad [R_0 = 1\ {\rm pc}]$$

How rapidly can the gas be expelled ?

$$E_{\rm bin} = \frac{GM_{\rm cl+g}^2}{R_0} = 8.6\times10^{40}\left(\frac{M_{\rm cl+g}}{M_\odot}\right)^2 \ {\rm erg}$$

$$t_{\rm cross} = 4.8\left(\frac{100\,M_\odot}{M_{\rm cl+g}}\right)^{\frac{1}{2}}\left(\frac{R_0}{\rm pc}\right)^{\frac{3}{2}}, \quad [R_0 = 1\ {\rm pc}]$$

$M_{\rm cl+g}$	$E_{\rm bin}$	$t_{\rm cross}$
$10^4\,M_\odot$	8.6×10^{48} erg	0.48 Myr
$10^5\,M_\odot$	8.6×10^{50} erg	0.15 Myr

How rapidly can the gas be expelled ?

$$E_{\rm bin} = \frac{G M_{\rm cl+g}^2}{R_0} = 8.6\times 10^{40} \left(\frac{M_{\rm cl+g}}{M_\odot}\right)^2 \ {\rm erg}$$

$$t_{\rm cross} = 4.8 \left(\frac{100\,M_\odot}{M_{\rm cl+g}}\right)^{\frac{1}{2}} \left(\frac{R_0}{\rm pc}\right)^{\frac{3}{2}}, \quad [R_0 = 1\ {\rm pc}]$$

$M_{\rm cl+g}$	$E_{\rm bin}$	$t_{\rm cross}$
$10^4\,M_\odot$	8.6×10^{48} erg	0.48 Myr
$10^5\,M_\odot$	8.6×10^{50} erg	0.15 Myr

Maeder (1990) stellar evolution models:

$m = 15\,M_\odot$ injects 3×10^{50} erg per 0.1 My

$m = 85\,M_\odot$ injects 3×10^{51} erg per 0.1 My

How rapidly can the gas be expelled ?

$$E_{\rm bin} = \frac{G M_{\rm cl+g}^2}{R_0} = 8.6\times 10^{40} \left(\frac{M_{\rm cl+g}}{M_\odot}\right)^2 \ {\rm erg}$$

$$t_{\rm cross} = 4.8 \left(\frac{100\,M_\odot}{M_{\rm cl+g}}\right)^{\frac{1}{2}} \left(\frac{R_0}{\rm pc}\right)^{\frac{3}{2}}, \quad [R_0 = 1\ {\rm pc}]$$

$M_{\rm cl+g}$	$E_{\rm bin}$	$t_{\rm cross}$
$10^4\,M_\odot$	8.6×10^{48} erg	0.48 Myr
$10^5\,M_\odot$	8.6×10^{50} erg	0.15 Myr

Maeder (1990) stellar evolution models:

$m = 15\,M_\odot$ injects 3×10^{50} erg per 0.1 My

$m = 85\,M_\odot$ injects 3×10^{51} erg per 0.1 My

$\Longrightarrow$ nebula disruption probably rapid

Pavel Kroupa: University of Bonn & Charles University

Further evidence *for* rapid gas-expulsion :

- Star-burst clusters in the Antennae $R \approx 4\,\mathrm{pc}$
  $t_{\rm cross} \approx 0.5\,\mathrm{Myr}$

  Gas-outflow velocities $v = 25 - 30\,\mathrm{km/s}$
  (Whitmore et al. 1999; Zhang, Fall & Whitmore 2001)

  → evacuation time-scale $\approx 0.2\,\mathrm{Myr} \approx t_{\rm cross}$

Further evidence *for* rapid gas-expulsion :

- Treasure Chest cluster : very compact with $R < 1\,\mathrm{pc}$
  age $\lesssim 0.2\,\mathrm{Myr}$

  HII region is expanding with $v \approx 12\,\mathrm{km/s}$ (Smith, Stassun & Baily 2004)

  → evacuation time-scale $\approx 0.1\,\mathrm{Myr}$

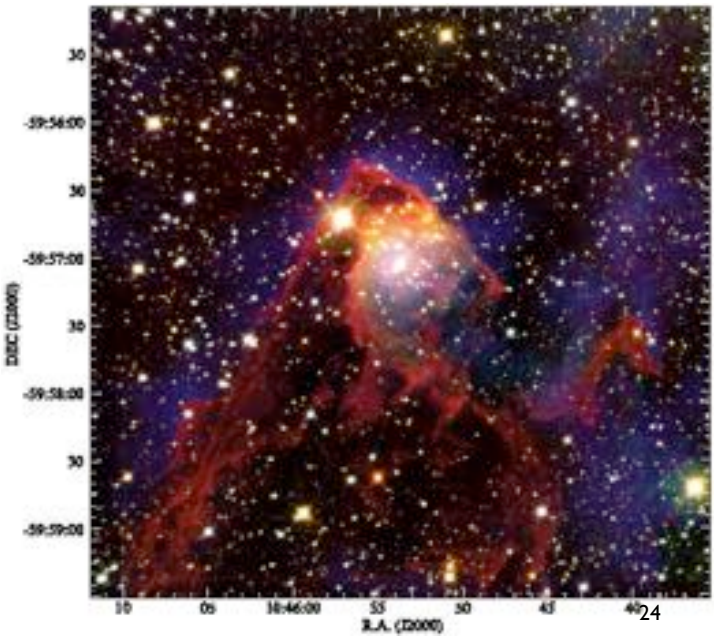

Thus, the examples
ONC, *Treasure Chest*, *R136*, *Antennae*
suggest that

"*in the presence of O stars, explosive gas expulsion may drive early cluster evolution independently of cluster mass*".

(Kroupa 2005)

But need realistic radiation--hydrodynamical simulations to help understand this problem better
(eg Ahmed Ali)

Realistic
N-body
experiments

Cluster reaction to sudden gas removal :

Similar work
by S. Pflazner.

Pavel Kroupa: University of Bonn & Charles University

Cluster reaction to sudden gas removal :

(Kroupa, Aarseth & Hurley 2001)

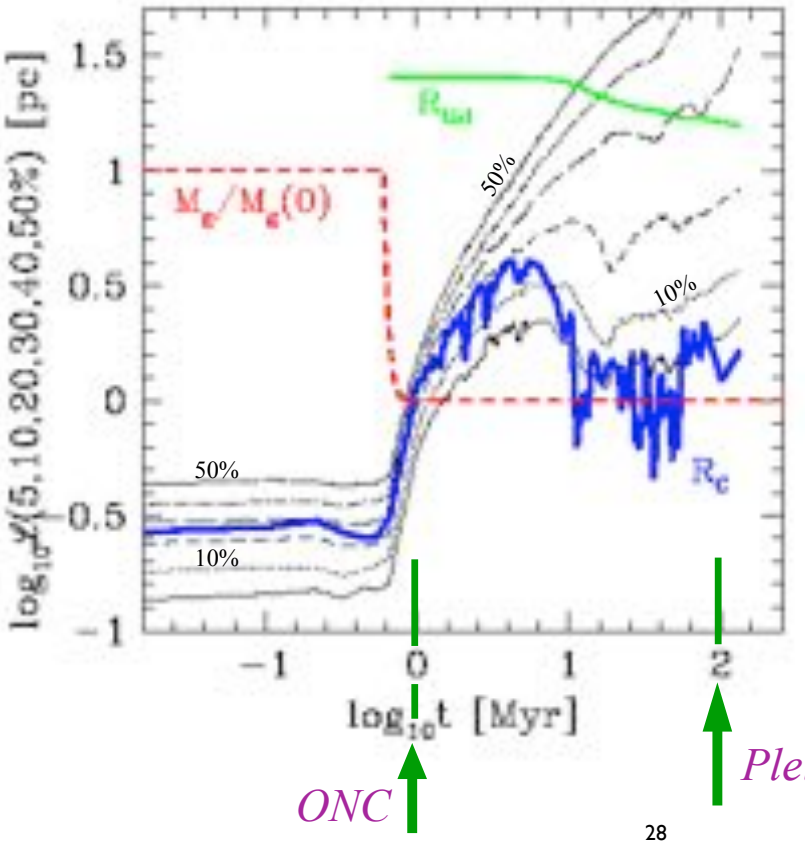

N-body models :

$N = 10^4$ stars + BDs

100 % binaries

$R = 0.4$ pc

$\rho_c = 10^5$ stars/pc^3

embedded phase = 0.6 Myr

$\tau_{\rm gas} \lesssim t_{\rm cross}$ (thermal)

$\epsilon = 1/3$

Pavel Kroupa: University of Bonn & Charles University

Early cluster evolution :

(Kroupa, Aarseth & Hurley 2001)

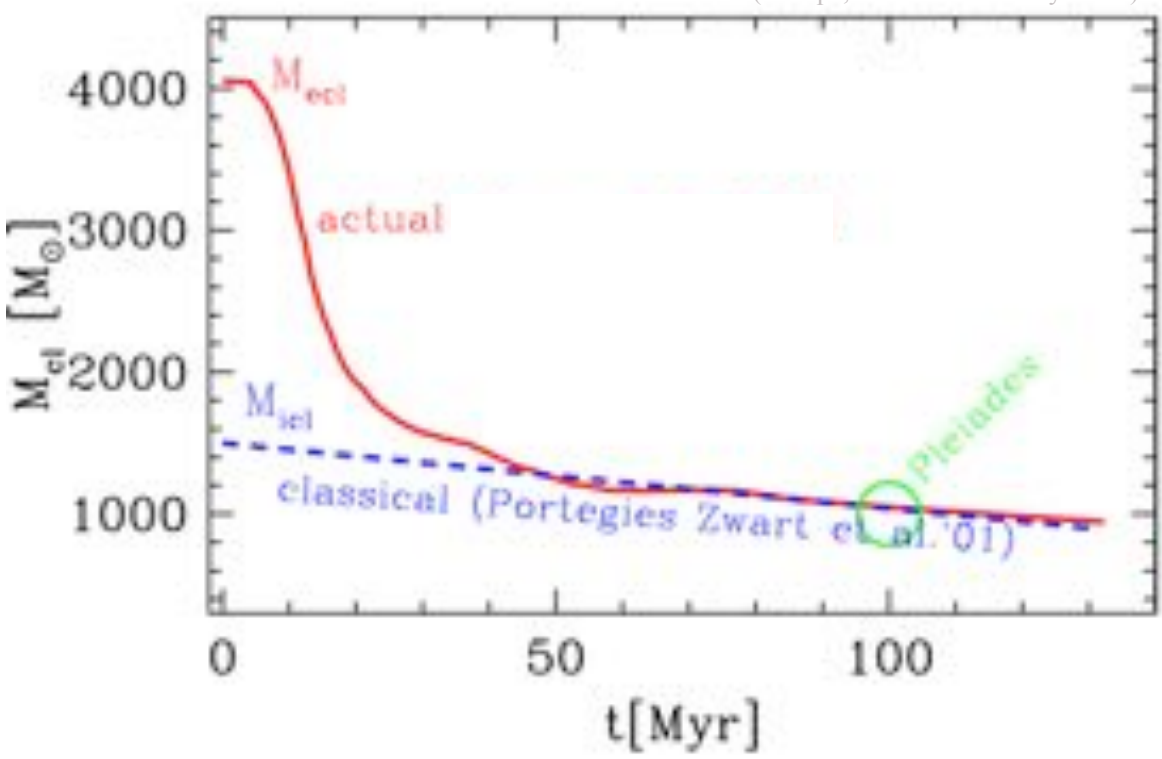

ONC

Pleiades ($\approx 1/3\ N$)
\+ *EP* ($\approx 2/3\ N$)

≈ 100 Myr

We thus have

ONC → *Pleiades* → *Hyades*

≈ 99 Myr ≈ 500 Myr

(Kroupa, Aarseth & Hurley 2001; Portegies Zwart etal. 2001; Kroupa 2005)

with an *inflation* in R .

Do
real clusters
show evidence
for this ?

Brandner, astro-ph/0803.1974

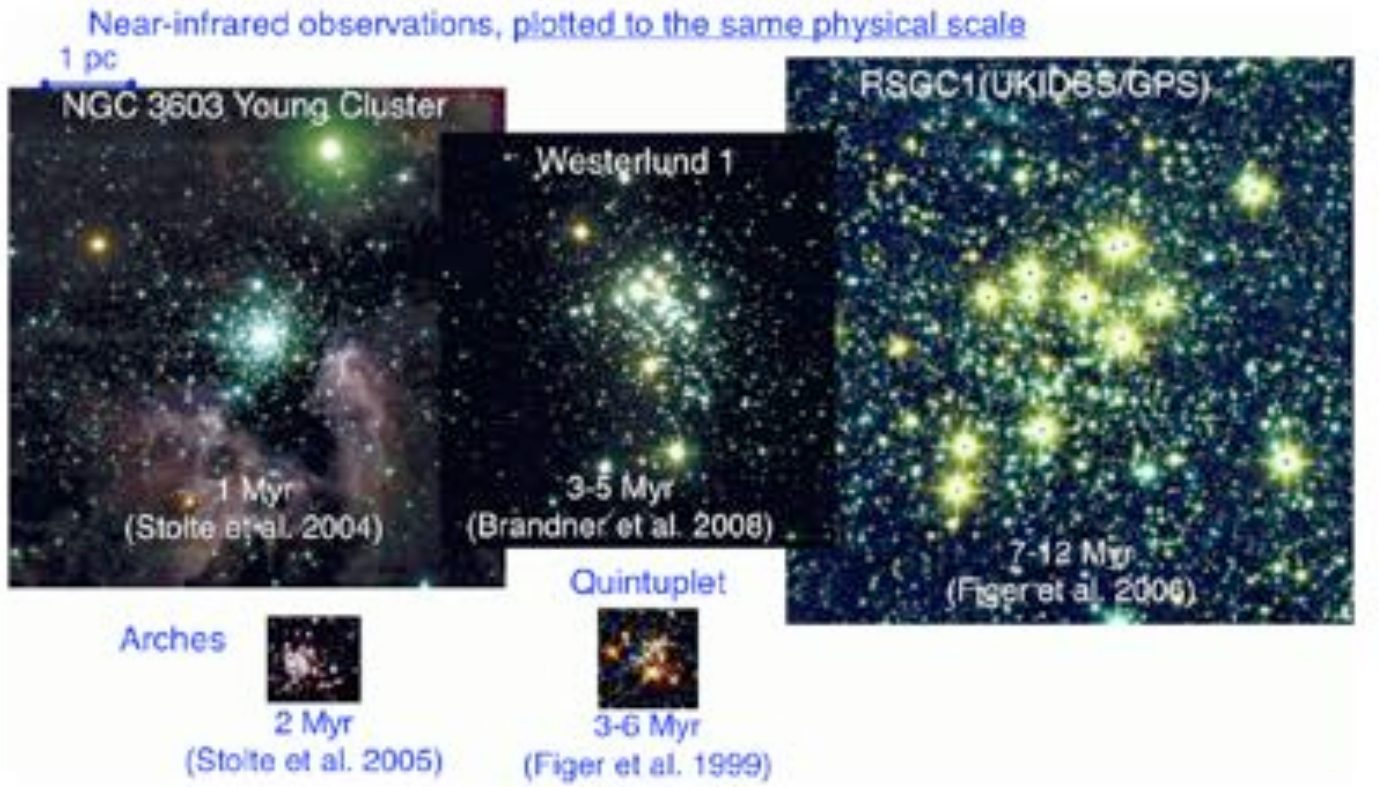

http://adsabs.harvard.edu/cgi-bin/bib_query?arXiv:1804.05075

Young star clusters in nearby molecular clouds

K V Getman ✉, M A Kuhn, E D Feigelson, P S Broos, M R Bate, G P Garmire

Monthly Notices of the Royal Astronomical Society, Volume 477, Issue 1, 11 June 2018, Pages 298–324,
https://doi.org/10.1093/mnras/sty473
Published: 22 February 2018 **Article history ▾**

Abstract

The SFiNCs (Star Formation in Nearby Clouds) project is an X-ray/infrared study of the young stellar populations in 22 star-forming regions with distances $\lesssim 1$ kpc designed to extend our earlier MYStIX (Massive Young Star-Forming Complex Study in Infrared and X-ray) survey of more distant clusters.

"The cloud-associated clusters are considerably smaller than the revealed clusters."

"Core radii increase dramatically from ~ 0.08 to ~ 0.9 pc over the age range 1–3.5 Myr."

Kinematics in Young Star Clusters and Associations with Gaia DR2

Michael A. Kuhn,[1] Lynne A. Hillenbrand,[1] Alison Sills,[2] Eric D. Feigelson,[3] and Konstantin V. Getman[3]

[1] *Department of Astronomy, California Institute of Technology, Pasadena, CA 91125, USA*
[2] *Department of Physics & Astronomy, McMaster University, 1280 Main Street West, Hamilton, ON L8S 4M1, Canada*
[3] *Department of Astronomy & Astrophysics, 525 Davey Laboratory, Pennsylvania State University, University Park, PA 16802, USA*

(Received July 5, 2018; Revised July 5, 2018)

Submitted to AAS Journals

ABSTRACT

The *Gaia* mission has opened a new window into the internal kinematics of young star clusters at the sub-km s^{-1} level, with implications for our understanding of how star clusters form and evolve. We use a sample of 28 clusters and associations with ages from ~1–5 Myr, where cluster members are already known from previous X-ray, optical, and infrared studies. Proper motions from *Gaia* DR2 reveal that 70% of these clusters show signs of expansion, with typical expansion velocities of ~0.5 km s^{-1}. Furthermore, in many expanding associations, there is a positive radial gradient in the expansion velocity. We consider NGC 6530 and the Orion Nebula Cluster (ONC) as prototypes for systems with and without expansion. Velocity dispersions among the sample clusters and associations range from $\sigma_{1D} = 1$–3 km s^{-1}. NGC 6530 is gravitationally unbound, with $\sigma_{1D} = 2.2 \pm 0.2$ km s^{-1} and expansion velocity 0.9 km s^{-1}, while the denser ONC is consistent with virial equilibrium, having $\sigma_{1D} = 1.8 \pm 0.1$ km s^{-1} and a Gaussian velocity distribution. The ONC also has a nearly constant velocity dispersion as a function of radius, but another non-expanding cluster, NGC 6231, has a velocity dispersion that decreases with radius. For those star-forming regions that contain multiple clusters or subclusters, we examine the kinematics of the individual groups and find that there is no evidence for ongoing coalescence of these groups. We compare our results to a cluster formation simulation, and comment on the implications for cluster assembly and the role of gas expulsion in cluster dissipation.

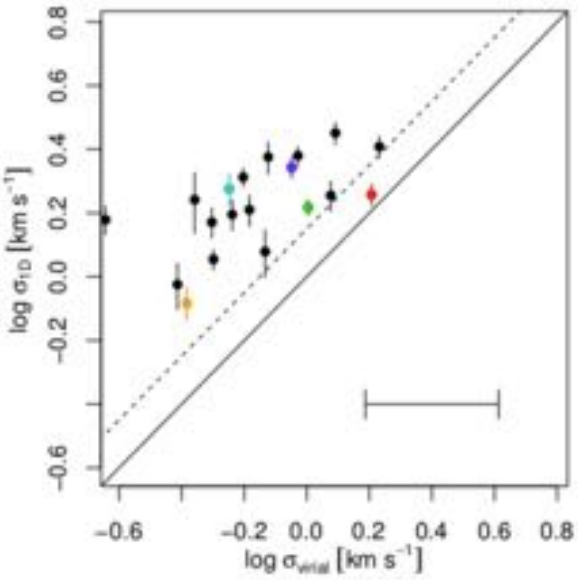

Figure 16. Virial velocity dispersion calculated using observed M_{cl} and r_{hm} versus observed velocity dispersion assuming a Plummer Sphere cluster model. Three non-expanding clusters are highlighted: the ONC (red), NGC 6231 (green), and NGC 2362 (orange). Two expanding clusters are highlighted: NGC 6530 (blue), and Cep B (cyan). The solid line shows the expected relationship for a cluster in virial equilibrium, while the dashed line shows the limit for a bound cluster. The large error bar shows how a factor of 2 uncertainty on cluster mass and cluster radius would affect σ_{virial}.

Rapid / violent *expulsion of residual gas* + *expansion* :

Taurus groups : the same
(Kroupa & Bouvier 2003)

ONC / Pleiades

(Kroupa, Aarseth & Hurley 2001)

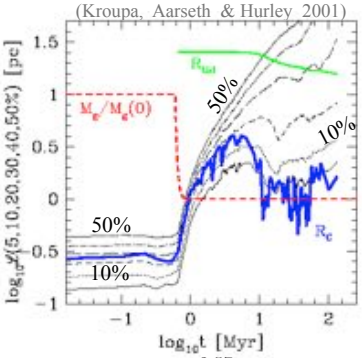

$M_{\rm ecl}(0) = 10^{3.57}\,M_\odot$
$r_{\rm h}(0) = 0.45$ pc

NGC 3603

(Banerjee & Kroupa 2014)

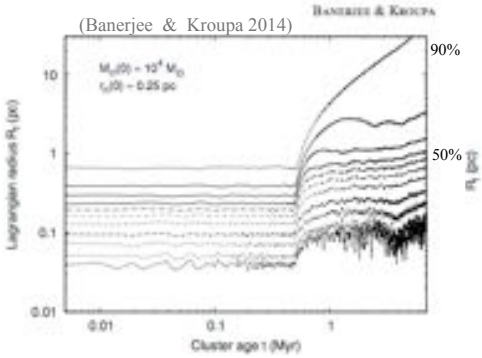

$M_{\rm ecl}(0) = 2\times10^4\,M_\odot$
$r_{\rm h} = 0.3$ pc

R136

(Banerjee & Kroupa 2013)

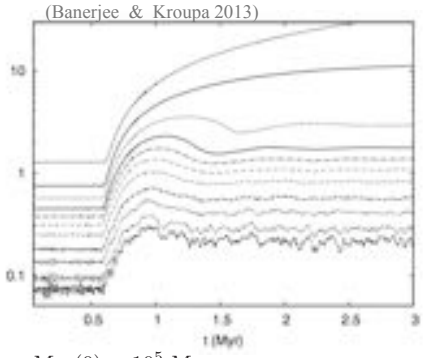

$M_{\rm ecl}(0) = 10^5\,M_\odot$
$r_{\rm h}(0) = 0.45$ pc

universal global residual gas values : $SFE = 0.33$ $\tau_{\rm M} = \dfrac{r_{\rm h}(0)}{10}$ Myr; (i.e. thermal time scale) $t_{\rm D} = 0.6$ Myr

Brinkmann et al. (2017)

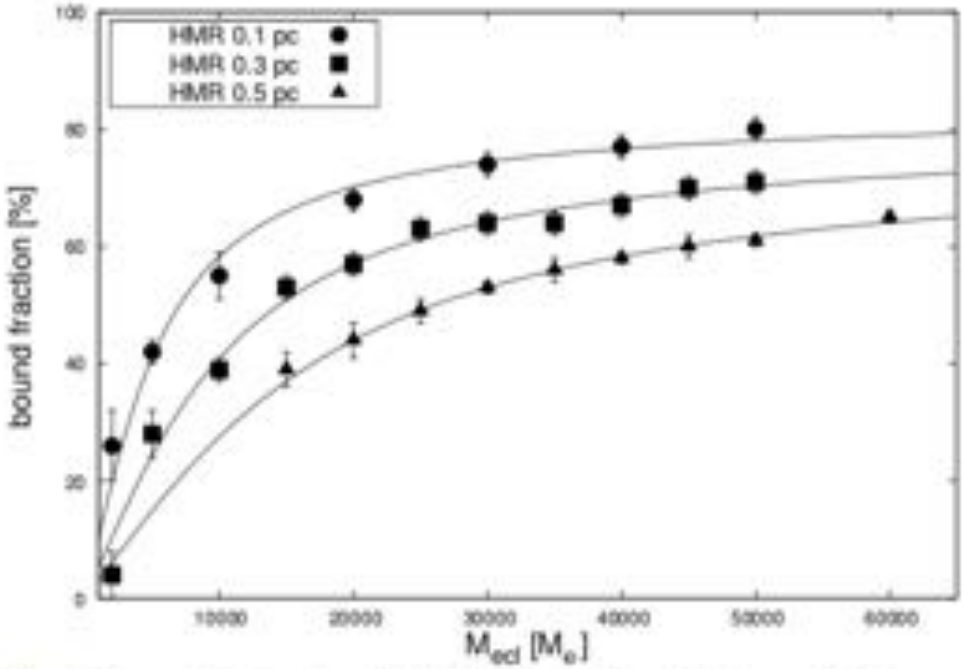

Fig. 1. Bound fraction for initial HMR of 0.1 pc, 0.3 pc and 0.5 pc as a function of initial cluster mass. The data points for 0.1 pc and 0.3 pc correspond to one run per mass, for 0.5 pc 3–6 are averaged.

Remnant cluster (e.g. open cluster) depends on mass of embedded cluster

But,
recent
results
for Orion...

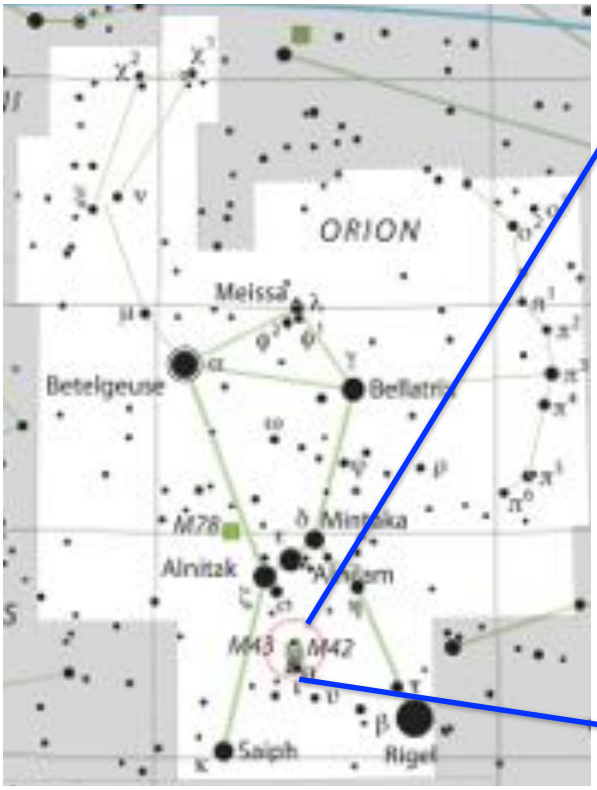

1752 publications between 1998 and 2018

Can we expect to observe something new?

Slide by Tereza Jerabkova, ESO, Garching

Slide by Tereza Jerabkova, ESO, Garching

A Tale of Three Cities:

OmegaCAM discovers multiple sequences in the color-magnitude diagram of the Orion Nebula Cluster

G. Beccari, M.G. Petr-Gotzens, H.M.J. Boffin, M. Romaniello, D. Fedele, G. Carraro, G. De Marchi, W.-J. de Wit, J.E. Drew, V.M. Kalari, C.F. Manara, E.L. Martin, S. Mieske, N. Panagia, L. Testi, J.S. Vink, J.R. Walsh, N.J. Wright

A&A, Letter to the Editor, 2017

The “smaller” 2.6-m VLT Survey Telescope captures bigger picture of the ONC region and revels unexpected results!

Pavel Kroupa: University of Bonn & Charles University

Do we need to revised star cluster formation?

Slide by Tereza Jerabkova, ESO, Garching

Star clusters form in one continuous event

feedback of massive stars truncates star formation and “destroys” gas and dust

Do we need to revised star cluster formation?

Slide by Tereza Jerabkova, ESO, Garching

Star clusters form in one continuous event

feedback of massive stars truncates star formation and “destroys” gas and dust

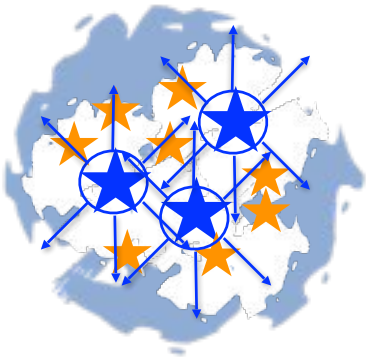

Pavel Kroupa: University of Bonn & Charles University

Do we need to revised star cluster formation?

Slide by Tereza Jerabkova, ESO, Garching

Star clusters form in one continuous event

feedback of massive stars truncates star formation and “destroys” gas and dust

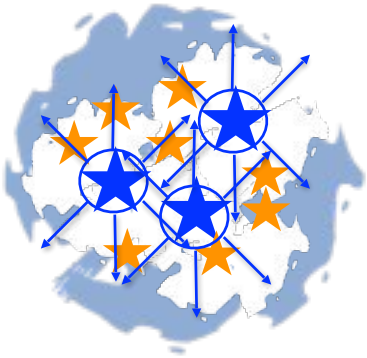

BUT: In the ONC three spatially distinct and age separated stellar populations have been found!

Pavel Kroupa: University of Bonn & Charles University

Do we need to revised star cluster formation?

Slide by Tereza Jerabkova, ESO, Garching

Star clusters form in one continuous event ?

feedback of massive stars truncates star formation and “destroys” gas and dust

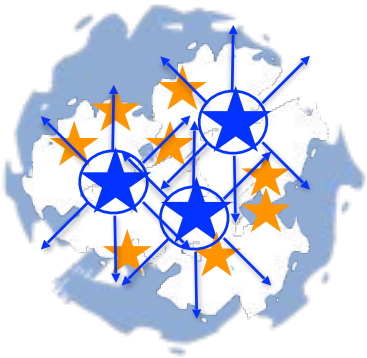

BUT: In the ONC three spatially distinct and age separated stellar populations have been found!

Pavel Kroupa: University of Bonn & Charles University

(Beccari et al. 2018, A&A)

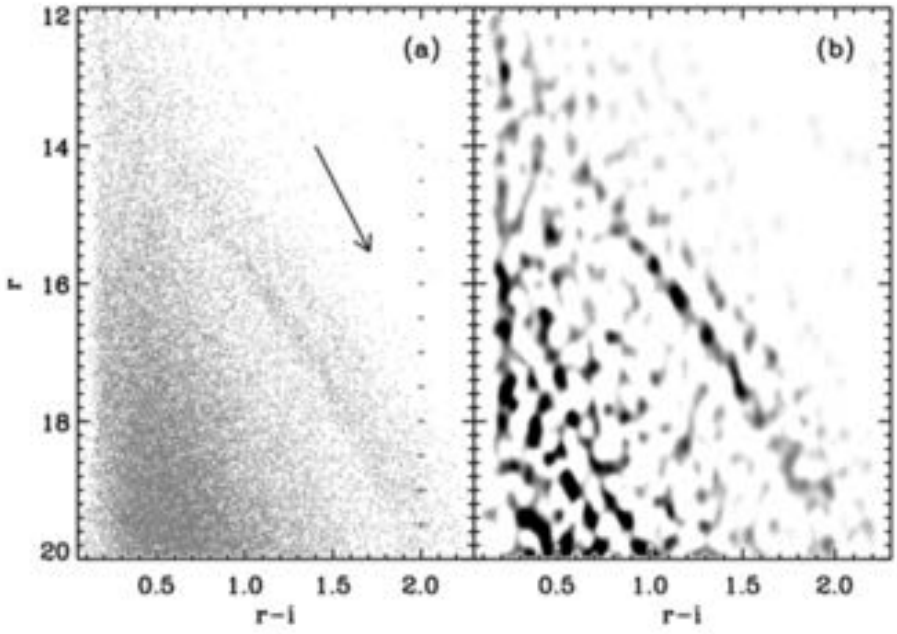

Fig. 1. **a)** The $(r - i)$, r color–magnitude diagram of a region of 1.5 radius centered on the ONC. The arrow represents a reddening vector for $A_v = 1.8$ (typical for Orion; Schlafly et al. 2014) and extinction curve with $R_v = 3.1$ (Cardelli et al. 1989). The photometric errors (magnitudes and colors) are indicated by black crosses; **b)** the same CMD shown in **a)** after unsharp masking.

(Beccari et al. 2018, A&A)

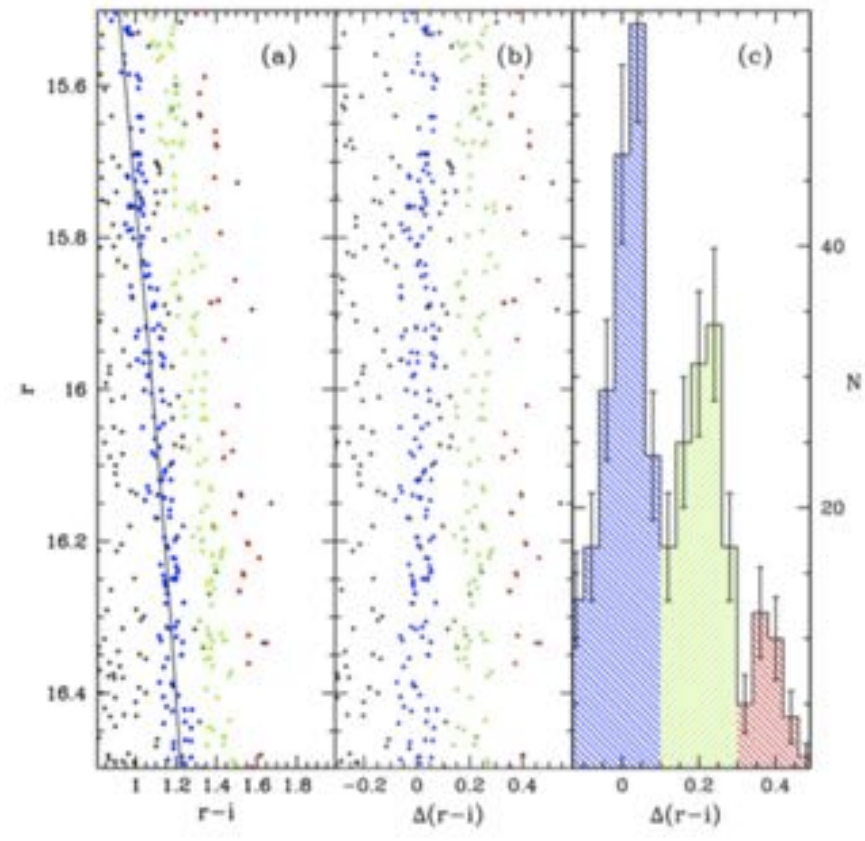

Fig. 2. **a)** Portion of the CMD zoomed on the PMS. The black line shows the mean ridge line of the blue population; **b)** rectification of the CMD shown in panel **a)**; **c)** histogram of the distance in $(r - i)$ color of the PMS stars from the mean ridge line of the bluest population.

(Beccari et al. 2018, A&A)

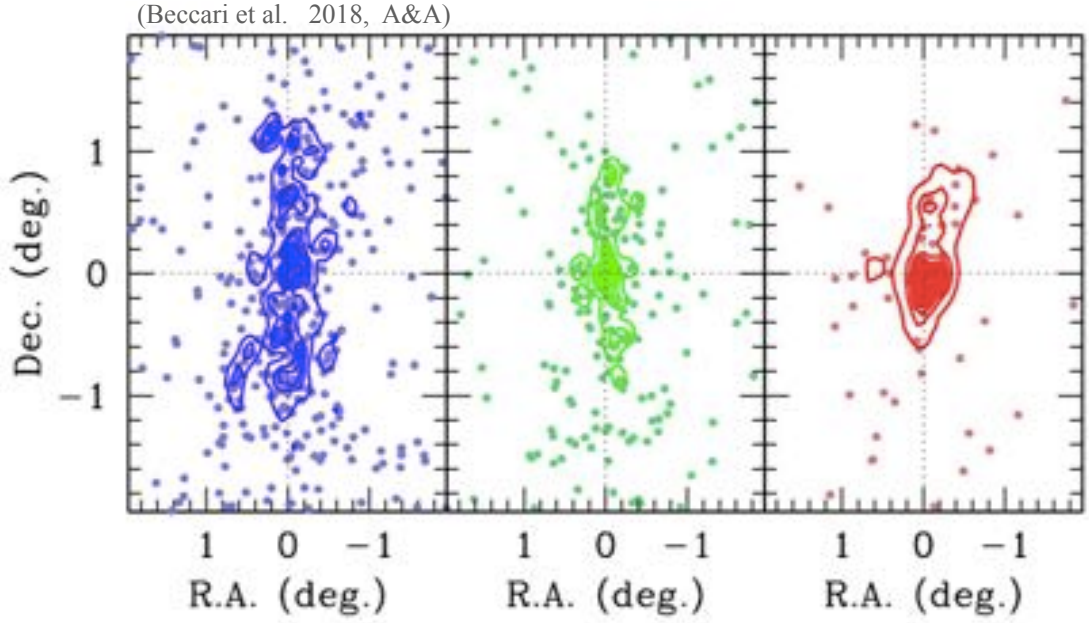

Fig. 3. Surface density of the three populations, old (in blue), young (in green), and very young (in red) together with the position of the stars. The plots have been centered on the ONC nominal center. All contours are normalized to the maximum value of the population itself. The location of the stars belonging to each population (solid dots) are also shown.

(Beccari et al. 2018, A&A)

Table 1. Properties of the three populations.

	Old	Young	Very young
Mean log age (yr)	6.46 ± 0.06	6.27 ± 0.09	6.09 ± 0.07
Mean age (Myr)	2.87	1.88	1.24
1-σ age interval (Myr)	2.51–3.28	1.55–2.29	1.08–1.53
5–95% interval (Myr)	2.30–3.58	1.37–2.60	1.04–1.63
Rotational velocity (km s^{-1})	14^{+6}_{-4}	25^{+25}_{-12}	35^{+36}_{-16}

How can these results be understood ?

A model

repeated stellar-dynamical termination
of
feedback-halted
filament-accretion model

The key may be
stellar-dynamical ejections

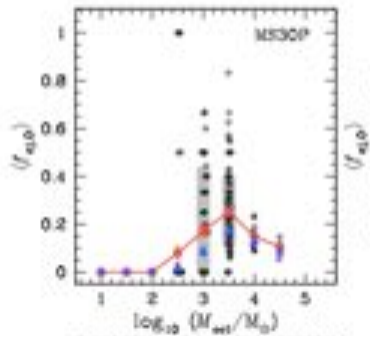

Oh et al. (2015)

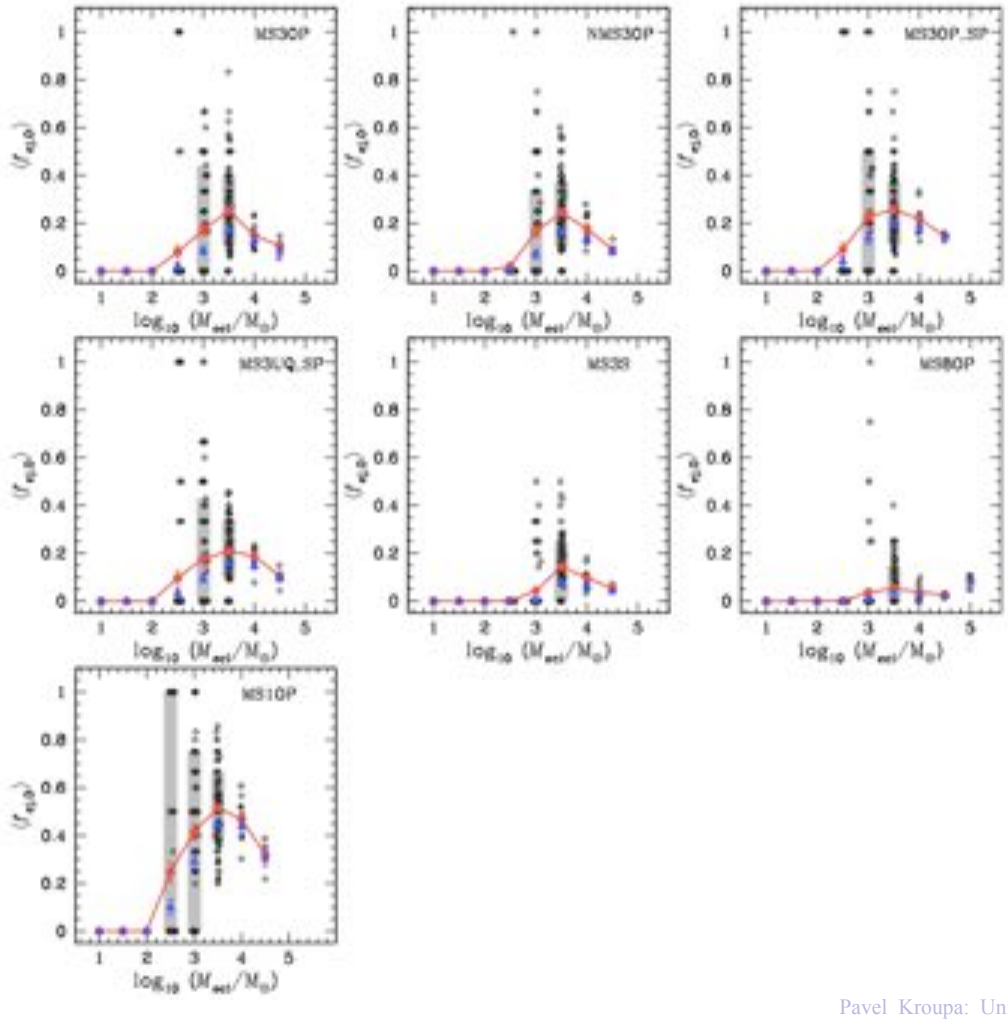

Oh et al. (2015)

Oh et al. (2015)

Figure 2. Ejection fraction of O-star systems as a function of cluster mass at 3 Myr. Red big circles are the average O star ejection fraction for each cluster mass and open circles are the values of individual clusters. The (red) solid lines are drawn by connecting the red points to guide the dependency of the ejection fraction on the cluster mass. Grey vertical bars indicate where the central 68 per cent of the data points lie (i.e., the points between 16 (lower) and 84 (upper) percentiles) for 10^3 and $10^{3.5}$ $M_\odot$ cluster models (for the MS1OP sequence $10^{2.5}$ $M_\odot$ clusters are included). Because more than 85 per cent of clusters with $M_{\rm ecl} = 10^{2.5}$ $M_\odot$ in each sequence except for clusters in the MS1OP sequence do not eject any O star, the grey bar is not plotted for this cluster mass with the exception for the MS1OP sequence. For more than 50 per cent of the 10^3 $M_\odot$ clusters of all sequences, except for the MS1OP sequence for which only 30 per cent of the cases, the O star ejection fraction is 0. Due to their small number of realisations and small spread of the ejection fraction, the grey bar is not necessary for clusters with $M_{\rm ecl} \geq 10^4$ $M_\odot$. Blue triangles are the average O star ejection fraction using 10 pc for the ejection criterion without applying a velocity criterion. The data for the 10^5 $M_\odot$ cluster model taken from the calculations by Banerjee et al. (2012) are marked with open stars in the MS8OP model sequence panel.

Table 1
List of N-body model sequences studied here.

Name	$r_{\rm h}$ (pc)	IMS	IBF	IPD	Pairing method
MS3OP	0.3	Yes	1	Kroupa95	OP
NMS3OP	0.3	No	1	Kroupa95	OP
MS3OP_SP	0.3	Yes	1	Sana et al.12	OP
MS3UQ_SP	0.3	Yes	1	Sana et al.12	uniform q dist.
MS3S	0.3	Yes	0	...	...
MS8OP	0.8	Yes	1	Kroupa95	OP
MS1OP	0.1	Yes	1	Kroupa95	OP

Note. — Names of model sequences and initial half-mass radii ($r_{\rm h}$) are listed in columns 1 and 2, respectively. Columns 3–6 present initial mass segregation (IMS), initial binary fraction (IBF), and initial period distribution (IPD) and pairing method used for massive binaries (primary mass ≥ 5 $M_\odot$).

Pavel Kroupa: University of Bonn & Charles University

Oh et al. (2015)

Figure 2. Ejection fraction of O-star systems as a function of cluster mass at 3 Myr. Red big circles are the average O star ejection fraction for each cluster mass and open circles are the values of individual clusters. The (red) so of the ejection fraction on the cluster mass. Grey vertical bars indicate where the centr nd 84 (upper) percentiles) for 10^3 and $10^{3.5}$ $M_\odot$ cluster models (for the MS1OP seq f clusters with $M_{\rm ecl} = 10^{2.5}$ $M_\odot$ in each sequence except for clusters in the MS1OP ter mass with the exception for the MS1OP sequence. For more than 50 per cent of t or which only 30 per cent of the cases, the O star ejection fraction is 0. Due to their s grey bar is not necessary for clusters with $M_{\rm ecl} \geq 10^4$ $M_\odot$. Blue triangles are the a ut applying a velocity criterion. The data for the 10^5 $M_\odot$ cluster model taken from th MS8OP model sequence panel.

Seungkyung Oh

List of N-body mo

Name	$r_{\rm h}$ (pc)	IMS	IBF	IPD	Pairing method
MS3OP	0.3	Yes			
NMS3OP	0.3	No	1	Kroupa95	OP
MS3OP_SP	0.3	Yes	1	Sana et al.12	OP
MS3UQ_SP	0.3	Yes	1	Sana et al.12	uniform q dist.
MS3S	0.3	Yes	0	...	...
MS8OP	0.8	Yes	1	Kroupa95	OP
MS1OP	0.1	Yes	1	Kroupa95	OP

Note. — Names of model sequences and initial half-mass radii ($r_{\rm h}$) are listed in columns 1 and 2, respectively. Columns 3–6 present initial mass segregation (IMS), initial binary fraction (IBF), and initial period distribution (IPD) and pairing method used for massive binaries (primary mass ≥ 5 $M_\odot$).

Pavel Kroupa: University of Bonn & Charles University

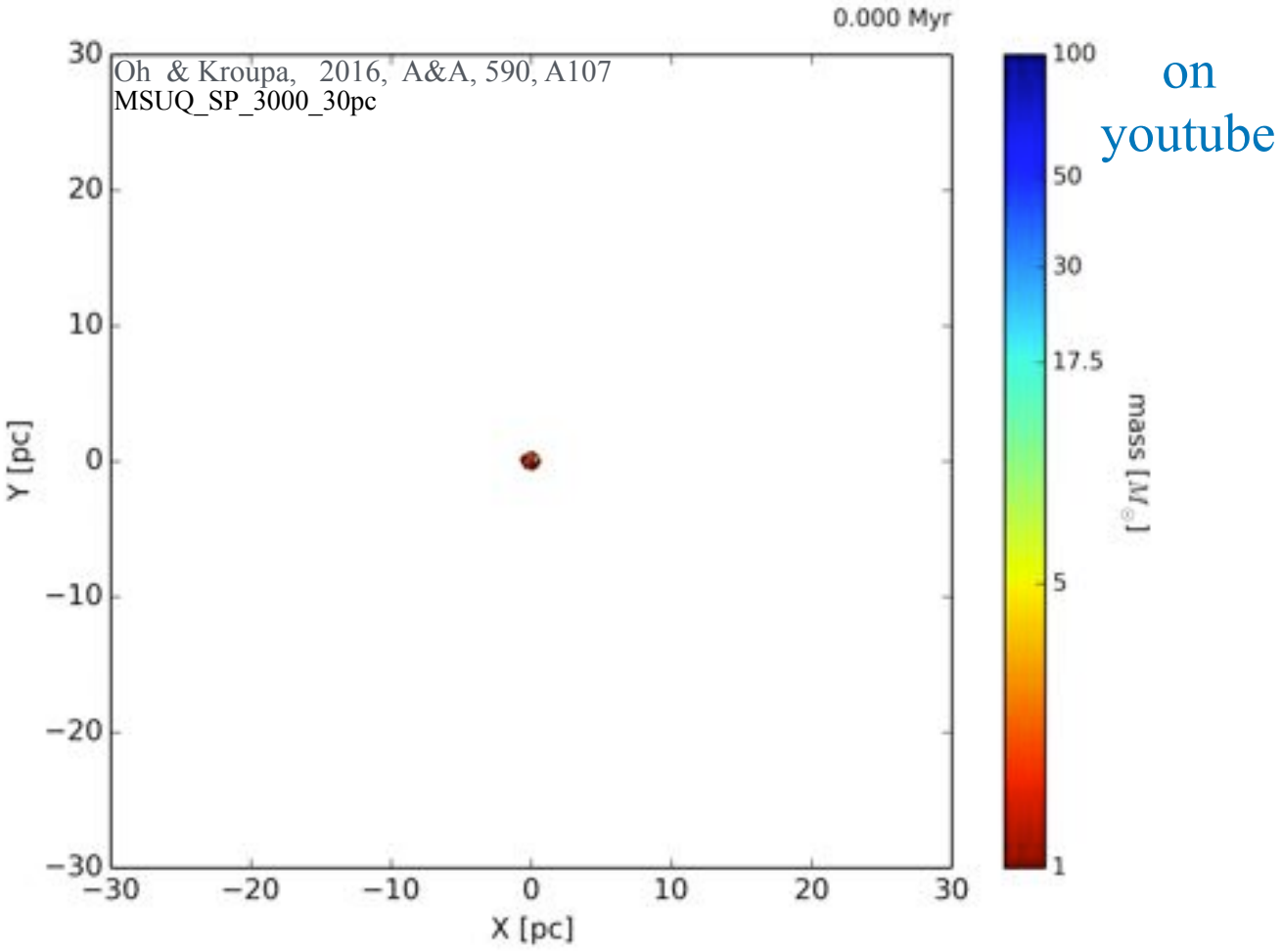

on youtube

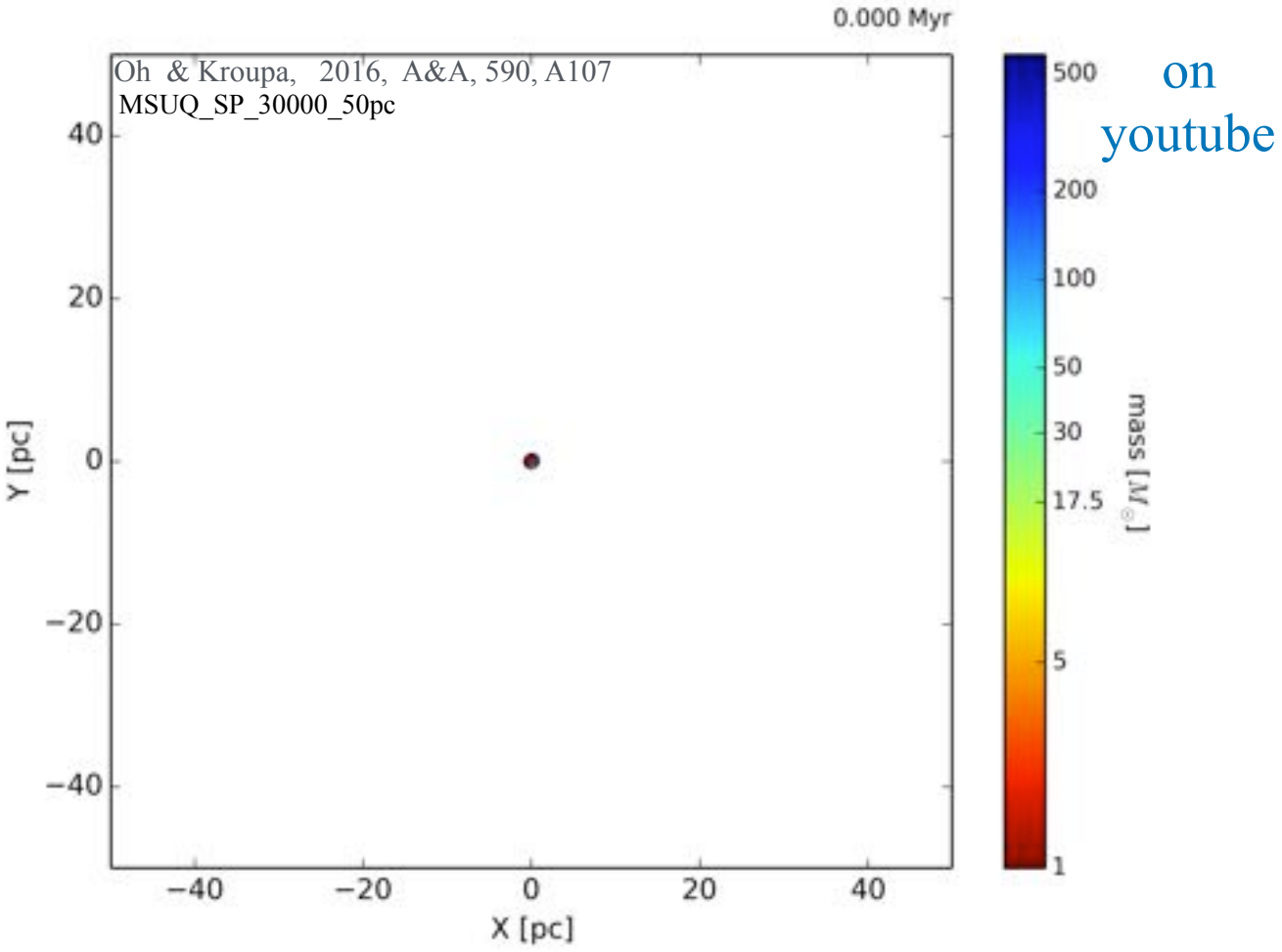

on youtube

Three stars can re-distribute their energies such that a stellar pair remains bound while the third carries off the surplus kinetic energy :

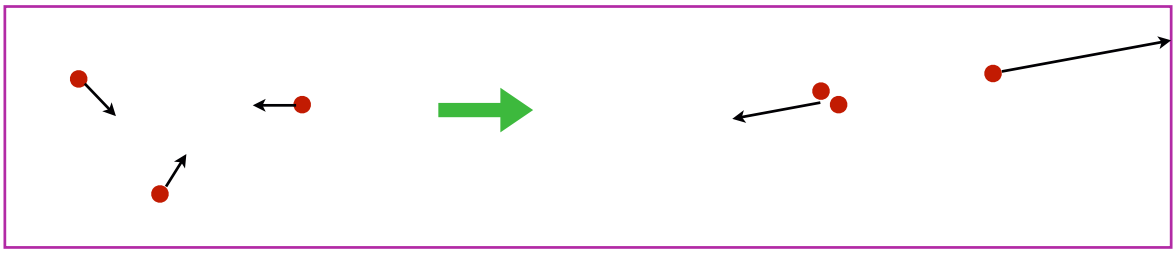

The *embedded clusters* contain high stellar densities, where such encounters are frequent.

Pre-existing stellar binaries enhance the likelihood of ejection events significantly.

Observation :

50 % of all O stars within 3kpc of Sun are outside clusters in OB associations;

10-25 % of all O stars are runaways (v>40 km/s);

2 % of B stars are runaways;

0.1-0.2 % of A stars are runaways.

(Gies & Bolton 1986)

→ Qualitative consistency with ***dynamical ejections*** from cluster cores. (Clarke & Pringle 1995; Pflamm & Kroupa 2006)

Most massive stars are in multiple systems;
(Goodwin et al. 2006, PPV; Chini et al. 2012; Sana et al. 2012)

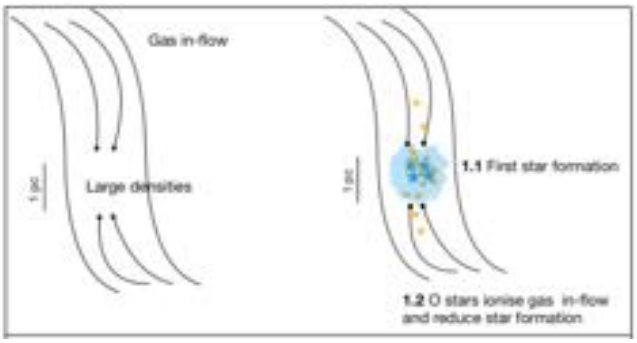

Kroupa, Jerabkova et al. (2018, A&A)

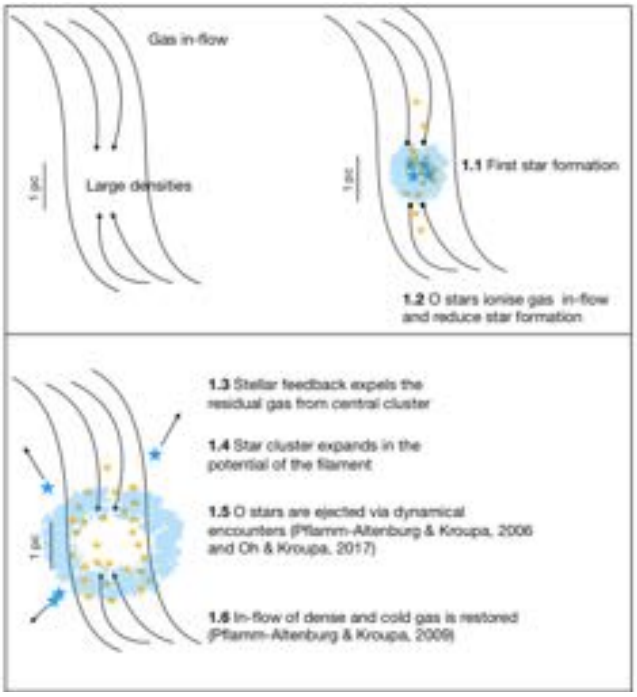

Kroupa, Jerabkova et al. (2018, A&A)

Pavel Kroupa: University of Bonn & Charles University

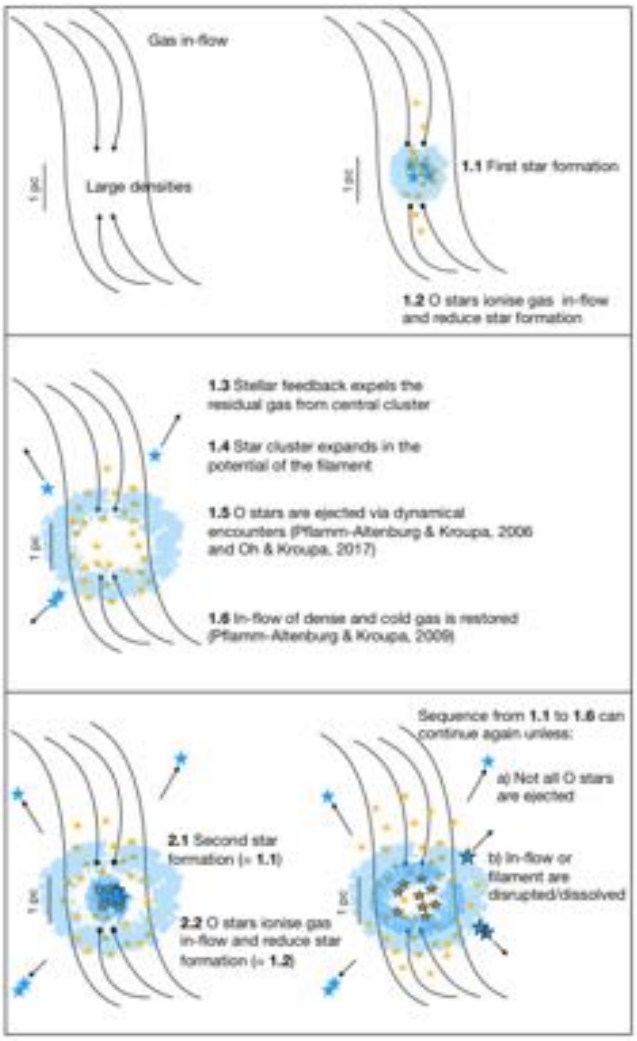

Kroupa, Jerabkova et al. (2018, A&A)

Formation of a stellar population : <1 Myr

If inflow sufficiently strong
(1000-6000 Msun/yr)
form 300-2000 Msun in stars
==> 2-few O stars

These terminate star formation but typically eject each other within 1 Myr.

Gas recombines (clouds live up to 10Myr) and new generation forms.

Inflow rates < 1000 Msun/yr)
form no O stars
==> one generation only

Inflow rates > 6000 Msun/yr)
form too many O stars
==> one generation only

Kroupa, Jerabkova et al. (2018, A&A)

The three O stars AE Aur, μ Col and ι Ori may be the stars ejected when the first ONC population formed.

Calculations of the trajectories of the stars AE Aur (spectral type O9.5V), μ Col (O9.5V) and ι Ori (O9III+B1III, binary) by Hoogerwerf et al. (2001); Gualandris et al. (2004) indicate that they all originated about 2.5 Myr ago from the ONC (see also the discussion in O'Dell et al. 2009).

Note that, if the IMF is an optimally sampled distribution function, then this first population will have had just such stars as the most massive ones.

Pavel Kroupa: University of Bonn & Charles University

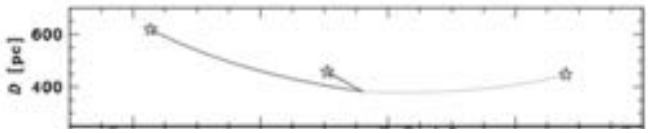

Hoogerwerf et al. (2001, A&A)

64 R. Hoogerwerf et al.: On the origin of the O and B-type stars with high velocities. II.

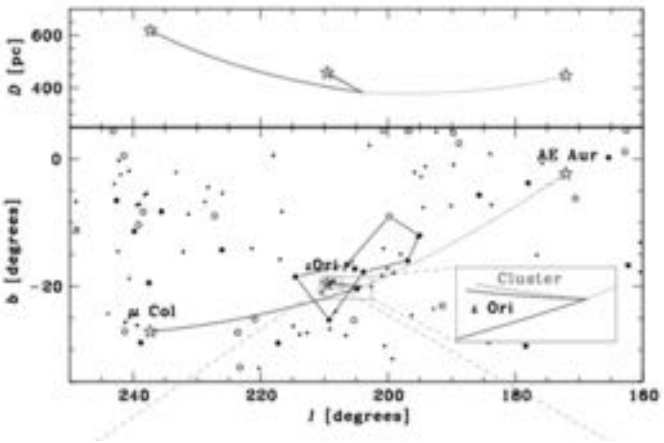

Hoogerwerf et al. (2001, A&A)

Pavel Kroupa: University of Bonn & Charles University

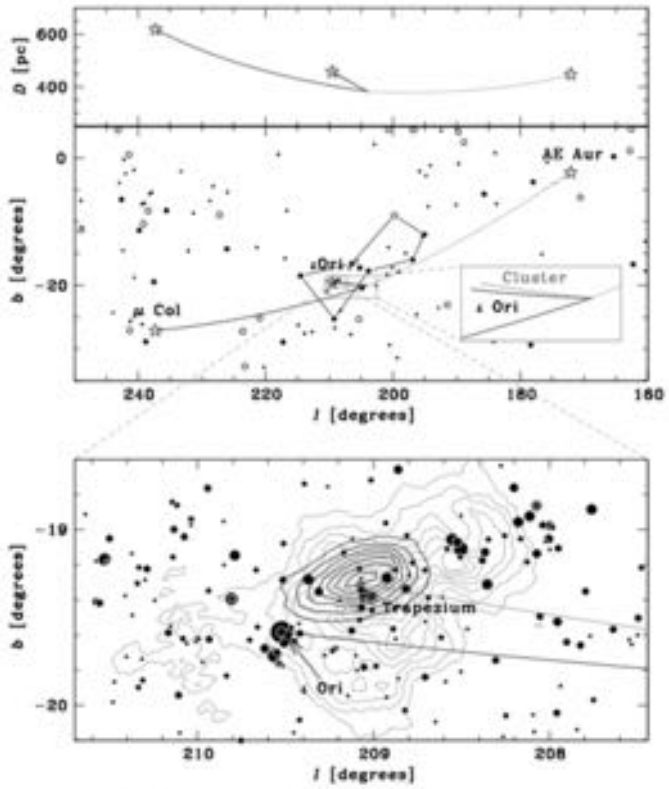

Hoogerwerf et al. (2001, A&A)

Fig. 11. *Top & middle:* Orbits, calculated back in time, of the runaways AE Aur (dotted line) and μ Col (solid line) and the binary ι Ori for one of the Monte Carlo simulations described in the text. The *top panel* shows the distance vs. Galactic longitude of the stars. The *middle panel* shows the orbits projected on the sky in Galactic coordinates. The starred symbols depict the present position of the three stars. The stars met ∼2.5 Myr ago. Using conservation of linear momentum, the orbit of the parent cluster (grey solid line, see *bottom up*) is calculated from the time of the assumed encounter to the present. The large circles denote all stars in the Hipparcos Catalogue brighter than $V = 3.5$ mag; filled circles denote O and B stars, open circles denote stars of other spectral type. The small circles denote the O and B type stars with $3.5 \text{ mag} \leq V \leq 5$ mag (cf. Fig. 1 in Blaauw & Morgan 1954). The Orion constellation is indicated for reference. *Bottom:* The predicted position of the parent cluster (black contours) together with all stars in the Tycho Catalogue (ESA 1997) in the field down to $V = 12.4$ mag. The size of the symbols scales with magnitude; the brightest star is ι Ori. The Trapezium and ι Ori are indicated. The black and dark grey lines are the past orbits of ι Ori and the Trapezium, respectively (see *top panel*). The triangle denotes the predicted present-day position of the parent cluster for this particular simulation. The grey contours display the IRAS 100 micron flux map, and mainly outline the Orion Nebula

Conclusions

Stars form as binaries (some as triples & quadruples) in compact (0.5pc) embedded clusters

These are very dynamic (cf Matthew Bate)

Feedback self-regulates the emergence of the stars

The embedded clusters expand significantly from gas removal **?**

But the ONC case shows very early cluster evolution to be complex

Small telescopes can yield big results !
(Tereza Jerabkova)

It is actually incredibly beautiful
how we can read-off from the sky
the detailed physical sequence of star formation
over a few Myr,
even down to individual stellar masses

Pavel Kroupa: University of Bonn & Charles University